Tuning exceptional points with Kerr nonlinearity

Shahab Ramezanpour* and Andrey Bogdanov
Department of Physics and Engineering, ITMO University, St. Petersburg 197101, Russia

(Received 13 October 2020; accepted 29 March 2021; published 15 April 2021)

An exceptional point (EP) is a singularity in non-Hermitian systems which exhibits exotic functionalities such as high sensitivity to external perturbations and fine selectivity of a laser mode arising due to the abrupt transition in the eigenvalue spectra. To achieve an EP, both the real and imaginary parts of two or several eigenfrequencies should coincide. Perturbations that appeared at the fabrication stage usually lift the degeneracy, and it impedes the experimental observation of EPs. In this work, we reveal that a Kerr-type nonlinearity can compensate for an initial distortion in resonant frequencies that is hardly avoidable in practice using the example of a pair of coupled ring resonators. We analyze the behavior of the eigenvalues and mode amplitudes in the vicinity of the second- and third-order EPs as a function of excitation amplitude. This work can help to improve the characteristics of the systems that support EPs, broadening their application to the domain of nonlinear photonics.

DOI: 10.1103/PhysRevA.103.043510

I. INTRODUCTION

Eigenfunctions and eigenvalues are the main characteristics of resonant systems (in acoustics, quantum mechanics, optics, etc.). At specific conditions, both the real and imaginary parts of some eigenvalues of a non-Hermitian system can degenerate, resulting in the appearance of so-called *exceptional points* (EPs). It is important to highlight that at an EP, eigenvalues and corresponding eigenvectors degenerate simultaneously. The abrupt phase transitions around this point in photonic systems lead to exotic functionalities such as unidirectional invisibility, laser mode selectivity, and sensitivity enhancement [1,2]. A more pronounced enhancement of sensitivity can be observed in the vicinity of high-order EPs when several complex eigenfrequencies degenerate [3].

In recent years, EPs in $\mathcal{PT}$-symmetric systems have attracted great attention as these systems can naturally host EPs. Hermitianness ensures that the Hamiltonian has real eigenenergies. However, as shown in Ref. [4], $\mathcal{PT}$-symmetric systems can also have entirely real eigenvalues even though they are non-Hermitian. However, beyond a critical condition, its eigenvalues become complex (broken $\mathcal{PT}$ symmetry), where this critical point has properties of the exceptional point. Under parity transformation $\hat{P}$, both momentum and spatial variables would be reversed ($\mathbf{p} \to -\mathbf{p}$, $\mathbf{r} \to -\mathbf{r}$), and time-reversal transformation $\hat{T}$ leads to the reverse of momentum and time variables, while spatial terms would be unchanged ($\mathbf{p} \to -\mathbf{p}$, $i \to -i$, $\mathbf{r} \to \mathbf{r}$). One calls a system $\mathcal{PT}$ symmetric when the commutation relation between the Hamiltonian and $\hat{P}\hat{T}$ operator, $[\hat{H}, \hat{P}\hat{T}] = 0$, is fulfilled. As a result, the potential of a one-dimensional [1D; $\mathbf{r} = (x, 0, 0)$], $\mathcal{PT}$-symmetric system obeys $V(x) = V^*(-x)$, which imposes gain and loss conditions on the coupled-resonator systems [5]. Although the $\mathcal{PT}$-symmetry approach was introduced in quantum mechanics, optics and photonics have been revealed as a suitable platform for the realization of such systems. In Ref. [6], a $\mathcal{PT}$-symmetric system was realized in a 1D inhomogeneous medium, where the wave equation is written as a Schrödinger-like equation and the potential in the Hamiltonian is related to the complex refractive index. The refractive index is distributed in a way that $n(x) = n^*(-x)$ (a necessary condition for a $\mathcal{PT}$-symmetric system); therefore, its real and imaginary parts should be even and odd functions of x, respectively. The system contains a ridge optical waveguide, where one half of it provides gain and the other half provides loss. The loss is controlled by the width of an additional strip layer made of Cr in the second half. The $\mathcal{PT}$-symmetric system in Ref. [7] consists of two coupled microtoroidal whispering gallery mode resonators, which are coupled to a different fiber-taper coupler. The gain in the first resonator is achieved by Er^{3+} doping, while the other resonator is passive (no-gain medium). Furthermore, the coexistence of nonlinearity and non-Hermiticity, in both optical systems and quantum mechanics, introduces another platform to investigate the EP and its functionalities such as unidirectionality and sensing [8–19]. We note that eigenvalues of Hermitian systems are entirely real, and the eigenmodes at the degenerate points are orthogonal. Therefore, these degenerate points cannot be considered an EP. Exceptional points can also be realized in non-Hermitian systems without gain and loss, therefore without parity-time symmetry, such as in coupled-resonator optical waveguides [20].

One of the main applications of EP-based systems is their responsivity (abrupt changes in their response around an EP versus a small perturbation) and sensitivity. Transmission spectra of a resonator, perturbed by a nanoparticle, show a splitting at the resonant frequency. This splitting is even larger in the resonator tuned to an EP [21]. This high responsivity

*ramezanpourshahab@gmail.com

can also be inferred from the eigenvalues of resonating systems. For instance, for a coupled resonator in the EP conditions, if we depict eigenvalues versus a parameter such as resonant detuning, $\omega_1 - \omega_2 = 2\epsilon$, the eigenvalues degenerate at $\epsilon = 0$. Small variation around $\epsilon = 0$ lifts the degeneracy since the eigenvalues have a sharp slope in the vicinity of $\epsilon = 0$. This perturbation can undesirably arise from fabrication imperfections. Therefore, to achieve the EP regime—a complete coincidence of the real and imaginary parts of resonant frequencies of two modes—precise control of geometrical and material parameters is necessary. However, unavoidable imperfections arising at the fabrication stage can impede reaching the EP regime. For example, the mismatch between the sizes of two coupled resonators or sidewall roughnesses leads to spectral detuning. This detuning can be compensated by photothermal heating such as a laser beam, which can act as both an excitation and heating source [3,7,22,23]. Here, we show that Kerr nonlinearity can also be incorporated to compensate for the possible spectral detuning; therefore, it does not need a heating scheme. In addition, even for a large value of contrast between the Kerr coefficients, the location of an EP would be tuned correspondingly. Moreover, compared to the heating procedure, Kerr nonlinearity is much faster. We propose Kerr nonlinearity as a fast low-profile configuration not only to overcome the difficulties associated with achieving the EP regime but to provide the possibility of creating an EP in a coupled resonator with two different resonances and eigenfrequencies. We note that, instead of Kerr nonlinearity, one may investigate phase transitions in the coupled resonators in the presence of saturable gain and loss nonlinearity [24,25].

Another challenge of EP-based sensors is related to the quantum noise arising from the fluctuation of the input signal and their non-Hermiticity, which can limit their precision [26,27]. However, [28] showed that, parametrically, the performance of the signal-to-noise ratio in EP sensors and their sensitivity can be enhanced. Furthermore, [29] studied the impact of a fluctuating Hamiltonian on the performance of EP-based sensors and proposed nonlinear effects such as gain saturation and adding uniform dissipation to the sensor and quantum-enhanced measurement [30] to improve their performance. Our work, which includes the nonlinear coefficient and field intensity in the Hamiltonian, can provide a suitable platform to investigate the sensitivity of EP-based sensors in the presence of quantum noise.

We consider the simplest example of the system supporting second- and third-order EPs and show that including Kerr nonlinearity can compensate initial spectral detuning. We develop a numerical method and solve the associated nonlinear eigenvalue problem. We demonstrate that by incorporating unequal nonlinear coefficients in the coupled resonators, the position of the EP can be tuned in the parameter space, and its location depends on the contrast between the nonlinear coefficients. It also gives us the opportunity to create the EP in coupled cavities with different resonant frequencies, where the difference between resonant frequencies can be compensated by nonlinearity containing unequal Kerr coefficients. Therefore, it provides an additional degree of freedom to control the phase transitions in the system.

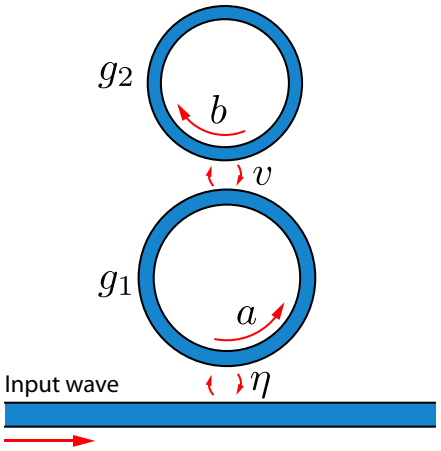

FIG. 1. Optical ring resonators with different Kerr materials coupled to a straight waveguide.

II. SECOND-ORDER EXCEPTIONAL POINT

An exceptional point can be observed theoretically and experimentally in a system containing gain and loss. The system can be, for example, a coupled pair of resonators in which one of the resonators contains gain and the other one has loss or two energy levels with loss [7,8]. The evolution of field amplitude of a coupled pair of resonators with complex frequencies Ω_1 and Ω_2 can be described by the eigenvalue problem:

$$\begin{pmatrix} \epsilon + g_1|a|^2 - 2i\delta & \upsilon \\ \upsilon & -\epsilon + g_2|b|^2 \end{pmatrix}\begin{pmatrix} a \\ b \end{pmatrix} = \mu\begin{pmatrix} a \\ b \end{pmatrix}. \quad (1)$$

This matrix equation describes such a system where the first equation corresponds to the loss, while the second equation is considered gain.

In Eq. (1), if we consider the complex resonant frequency of the resonators $\Omega_1 = \omega_1 - i\gamma_1 = \epsilon - 2i\delta$ and $\Omega_2 = \omega_2 - i\gamma_2 = -\epsilon$, we can write $\Omega_1 - \Omega_2 = (\omega_1 - \omega_2) - i(\gamma_1 - \gamma_2) = 2\epsilon - i2\delta$. Therefore, 2ϵ and 2δ are the differences between the (real) resonant frequencies and loss of resonators, υ is the coupling rate between the resonators, μ is the eigenvalue of the coupled system, a and b are the field amplitudes, and g_1 and g_2 are the Kerr nonlinear coefficients of the first and second resonators with loss and gain, respectively. This form of the matrix equation can be used for the description of different systems from quantum mechanics, with the nonlinear Schrödinger equation applied to a two-level system with loss [16,31], to photonics, with the coupled mode theory approach containing Kerr nonlinearity [18,32,33]. One of the simplest examples describing the system of equations (1) is two optical ring resonators with different Kerr materials coupled to a waveguide, as schematically shown in Fig. 1. In Fig. 1, the radii of the resonators are considered different in order to show that the EP can happen in this system by attributing unequal Kerr coefficients (g_1, g_2) to the rings.

For the linear case, we should put $g_1 = g_2 = 0$ in Eq. (1); therefore, the eigenvalues of this equation can be calculated

analytically:

$$\begin{vmatrix} \Omega_1 - \mu & \upsilon \\ \upsilon & \Omega_2 - \mu \end{vmatrix} = 0. \tag{2}$$

The eigenvalues of this system are

$$\mu = \frac{\Omega_1 + \Omega_2 \pm \sqrt{(\Omega_1 - \Omega_2)^2 + 4\upsilon^2}}{2}. \tag{3}$$

To have an EP, the square-root term should be zero, which imposes the conditions $\omega_1 - \omega_2 = 2\epsilon = 0$ and $\gamma_1 - \gamma_2 = 2\delta = \pm 2\upsilon$ for the real value of υ.

EP-based systems are highly responsive to small perturbations around an EP, leaving them vulnerable to unwanted perturbations. For instance, in the above EP conditions, for $\epsilon \neq 0$ (i.e., when there is resonant detuning in the coupled resonators), the degeneracy would be lifted. In the following sections, we show that even for $\epsilon \neq 0$, we can have an EP due to the nonlinearity, and resonance detuning can be compensated. Furthermore, studying the sensitivity of nonlinear EPs in the presence of quantum noise can be intriguing since their Hamiltonian contains field intensity, and tuning the nonlinear coefficients can be used as leverage to reduce the effect of external and internal noise.

Numerical method

The EP can occur in nonlinear non-Hermitian systems such as in a two-level system described by the nonlinear Schrödinger equation [8–13]. To solve a nonlinear eigenvalue problem, different methods can be used, for example, polar representation [14,15], incorporating the Stokes parameters and angular momentum operators [16–19]. These methods may be cumbersome or limited to specific considerations, for instance, that one should know both pumping and resonant frequencies of cavities or that nonlinear coefficients in the matrix equation should be equal. Here, we propose another method which is based on the self-consistent field approach and also takes into account the behavior of the eigenfunctions in the iteration process. This method can be utilized in a wide variety of nonlinear eigenvalue problems and also the higher-order nonlinear matrix equation. To demonstrate the efficiency of this method, we use unequal nonlinear coefficients in the 2×2 and 3×3 nonlinear matrix equations (which can be realized in coupled resonators with different Kerr materials), and we could observe that the EP can be tuned with respect to parameter space.

To calculate the eigenvalues of the nonlinear eigenvalue problem in Eq. (1), with respect to parameter space ϵ, we use a method similar to the self-consistent-field method [34] in two stages. First, for large values of $|\epsilon|$, the problem is close to the linear case (in the eigenvalue problem, $|a|^2$ and $|b|^2$ represent the probability densities of energy levels; therefore, they are smaller than unity, and for $|\epsilon| \gg g_1, g_2$, in the matrix equation, the terms $g_1|a|^2a$ versus ϵa and $g_2|b|^2b$ versus ϵb can be ignored). Therefore, in this region, we consider the linear case ($g_1 = g_2 = 0$) and find eigenvalues and eigenfunctions of Eq. (1). Then, we use these eigenfunctions in the nonlinear eigenvalue problem [Eq. (1)] and find new eigenfunctions. We repeat this iteration until the result converges to a specific threshold (to get a better convergence, we may use the average of the newly calculated eigenfunctions and the previous one as the next iteration value). For lower values of $|\epsilon|$, we use the converged result of the previous step as the initial value and repeat the process. Figure 2 shows the real and imaginary parts of μ for $\delta = \upsilon = 1$ and $g_1 = g_2 = 1.8$ (the values of g_1 and g_2 are chosen arbitrarily, while the values of δ and υ are equal, which is a condition of an EP). In Fig. 2 and other figures, each branch of the real part of the eigenvalue and its corresponding imaginary part are shown by different colored arrows. It shows some discontinuities at four points (where the four branches should continue their route and coincide at the EP). Meanwhile, near the EP, there are some divergences in the result (shown by dashed circles). In this region, where the nonlinearity becomes more significant (with decreasing absolute value of ϵ), the direction of the functions related to the real and/or imaginary parts changes, which causes the divergence near the EP. By defining the additional parameters Δ_i in the eigenfunctions, we force the eigenfunctions to continue their rate of change near the EP and therefore prevent the result from the divergence.

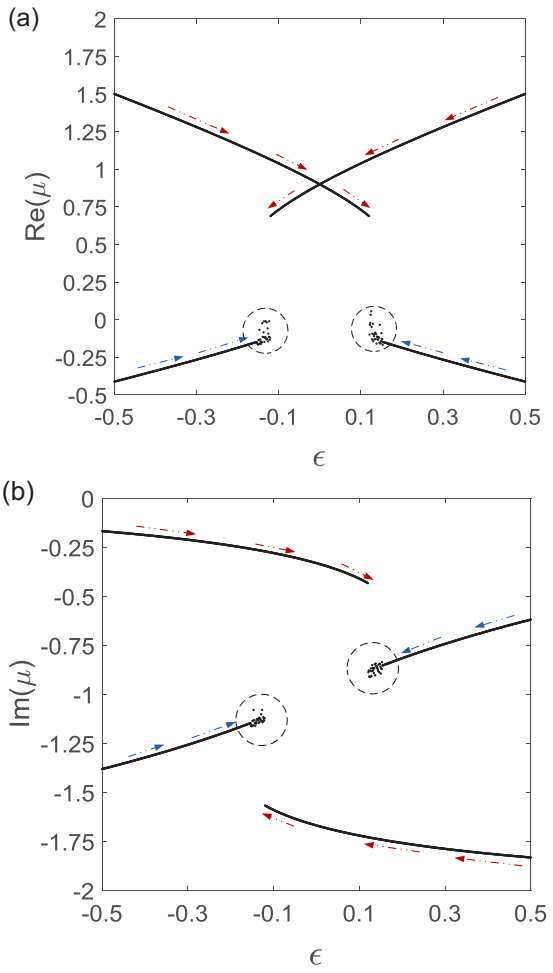

FIG. 2. First stage to calculate (a) real and (b) imaginary parts of eigenvalues of a 2×2 nonlinear matrix equation, numerically.

In the second stage, in order to resolve the discontinuities (and divergences) in Fig. 2, we study the behavior of the eigenfunctions near this region. Accordingly, we define the parameters Δ_1, Δ_2, Δ_3, Δ_4 and set a range of values for them

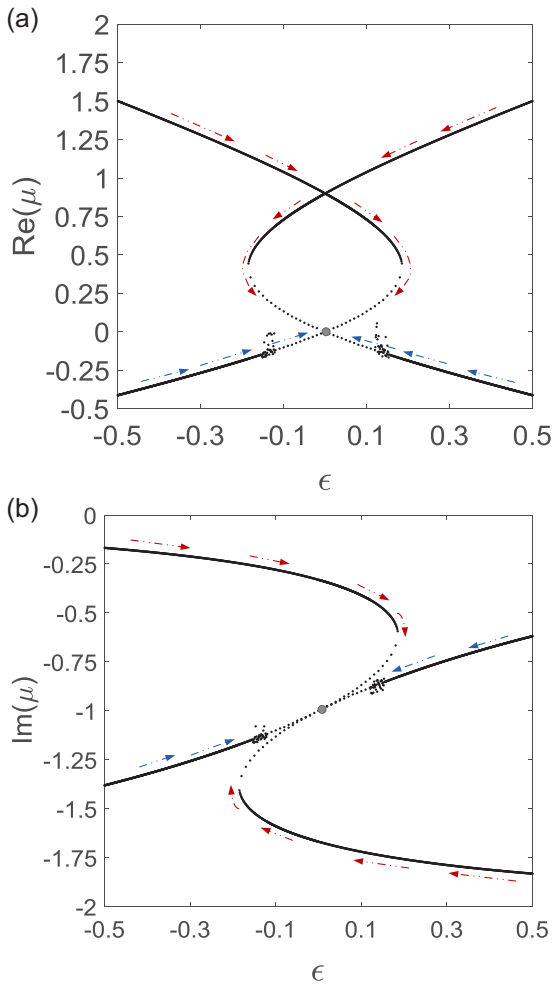

FIG. 3. (a) Real and (b) imaginary parts of eigenvalues of a 2×2 nonlinear matrix equation containing EPs with equal Kerr coefficient nonlinearity.

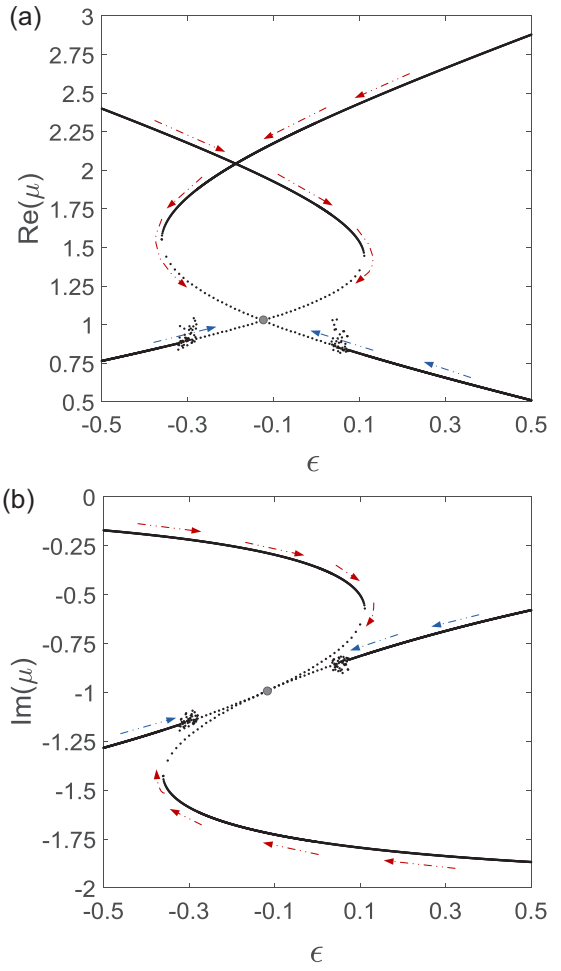

FIG. 4. The EP in the 2×2 matrix equation can be tuned by the contrast between the Kerr nonlinearity. Moreover, close to the EP, (a) real parts of eigenvalues coalesce, while (b) their imaginary parts depart.

and consider the eigenfunction $(a_c + \Delta_1 + i\Delta_2, b_c + \Delta_3 + i\Delta_4)$ as the initial value of the next step. First, we consider the parameters Δ_1, Δ_2, Δ_3, Δ_4 as very small values compared to the changing rate of the eigenfunctions in each step. If it cannot not converge to a specific value through the iteration method, they would increase gradually. Figure 3 shows the result which is obtained after these two stages, which completely matches analytical results in Refs. [8,35] (the EPs in Fig. 3 and other figures are shown by gray dots).

Here, we investigate the result when the Kerr nonlinear coefficients (g_1, g_2) are unequal. A system with unequal nonlinear coefficients may be realized in multiple resonators with materials with different Kerr constants [36]. Figure 4 depicts eigenvalues of Eq. (1) with $g_1 = 2.3$, $g_2 = 1.8$. Figure 4 shows that the exceptional point occurs at $\epsilon = -0.12$. By changing the values of nonlinear coefficients, EP can be tuned with respect to ϵ. Another feature of Fig. 4 is that the result is asymmetric with respect to the EP. Slightly lower than the EP, at $\epsilon = -0.18$, the real parts of the eigenvalues coalesce, while their imaginary parts depart. Therefore, the nonlinear coefficients can be utilized as leverage to tune the photonic system between different phases, as well as the location of the EP. In linear systems, as well as in nonlinear systems with equal Kerr nonlinearities, EPs occur at $\epsilon = 0$, where the real parts of the resonant frequencies are equal. However, in Fig. 4, the EP occurs at a nonzero value of ϵ; therefore, the difference between the resonant frequencies (due to the imperfections, etc.) can be compensated by an appropriate contrast between the nonlinear coefficients.

III. THIRD-ORDER EXCEPTIONAL POINT

Higher-order exceptional points in a photonic system may be utilized in some applications such as sensitivity enhancement [3,37]. In this section we investigate the effect of nonlinearity on such systems. Figure 5 shows eigenvalues of a 3×3 matrix equation, Eq. (4), which corresponds to three rings, which act as gain, a neutral ring, and loss (with $+i\gamma$, $+i0$, and $-i\gamma$, respectively). Figure 5 depicts an example for $\kappa = 1$ and $\gamma = \sqrt{2}\kappa$ (the condition that a third-order EP can occur). It shows that third-order EPs occur at $\epsilon = 0$, where six

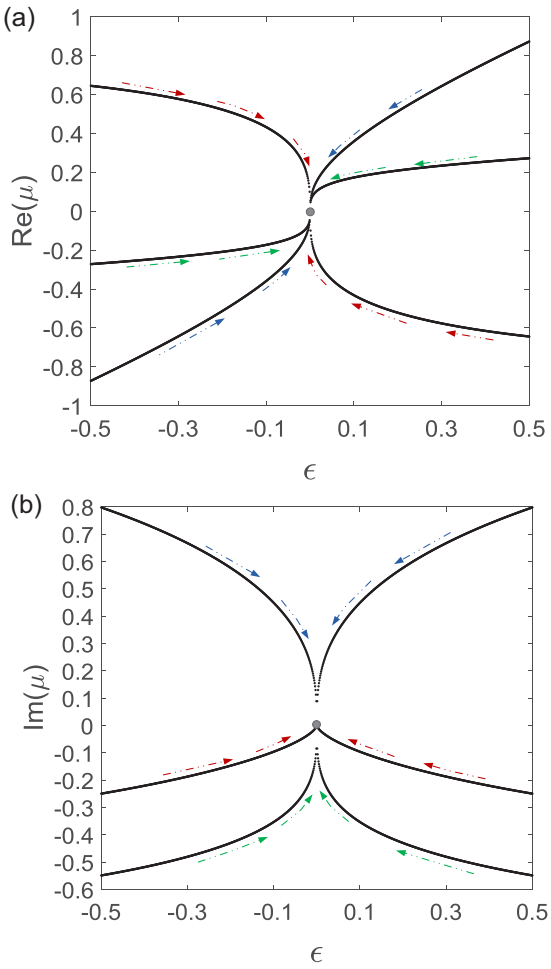

FIG. 5. The EP in the linear 3×3 matrix equation: (a) real part and (b) imaginary parts of the eigenvalues.

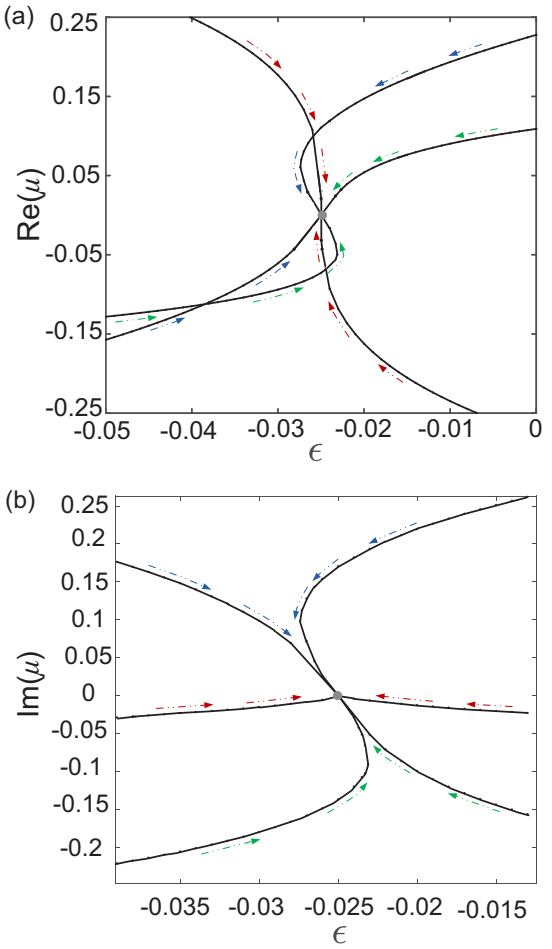

FIG. 6. The EP can be tuned by the nonlinear coefficient. Furthermore, (a) the real part coalesces at two points below and higher than the EP, while (b) the imaginary parts depart.

branches coalesce:

$$\begin{pmatrix} i\gamma + \epsilon + g_1|a|^2 & \kappa & 0 \\ \kappa & g_2|b|^2 & \kappa \\ 0 & \kappa & -i\gamma + g_3|c|^2 \end{pmatrix} \begin{pmatrix} a \\ b \\ c \end{pmatrix} = \mu \begin{pmatrix} a \\ b \\ c \end{pmatrix}. \tag{4}$$

Figure 6 shows the result for the nonlinear case with $g_1 = 0.1$, $g_2 = g_3 = 0$. It is obtained with a method similar to that above, although we have to deal with a higher order of matrix and a higher number of branches. Figure 6 shows that third-order EP occurs at $\epsilon = -0.025$.

Figure 6 reveals that the number of eigenvalues near the EP can be up to 5. Moreover, the real parts of the eigenvalues coincide at around $\epsilon = -0.026$ and $\epsilon = -0.0245$, while their imaginary parts depart. These points, which have distances of 0.001 and 0.0005 from the EP, could be the source of additional resonances in the transmission and reflection coefficients in photonic systems, which can be tuned by the nonlinear coefficients as well as the location of the EP. The EP occurring at a nonzero value of ϵ, which is related to the difference between the resonant frequencies of resonators, implies that the difference between resonant frequencies can be compensated by imposing unequal nonlinear coefficients on the system.

IV. IDEAL $\mathcal{PT}$-SYMMETRIC RESONATORS

In the previous sections, we analyzed the eigenvalue problem; however, in practice, we measure the response of the system to an external signal. In this section, we investigate the mode amplitudes in ideal $\mathcal{PT}$-symmetric coupled resonators at which the gain in the active resonator is equal to the loss in the passive one. For this purpose, we write the coupled mode theory for coupled resonators with unequal Kerr nonlinearities (Fig. 1) as

$$\omega a = (\omega_0 + \epsilon + g_1|a|^2 - i\delta)a + \upsilon b - \eta s_i, \tag{5a}$$

$$\omega b = \upsilon a + (\omega_0 - \epsilon + g_2|b|^2 + i\delta)b, \tag{5b}$$

where ω and s_i are the frequency and amplitude of the source, η is mutual coupling between the source waveguide and ring resonator, and $\omega_0 + \epsilon$ and $\omega_0 - \epsilon$ are the resonant frequencies of the first and second rings, respectively. Therefore, mode

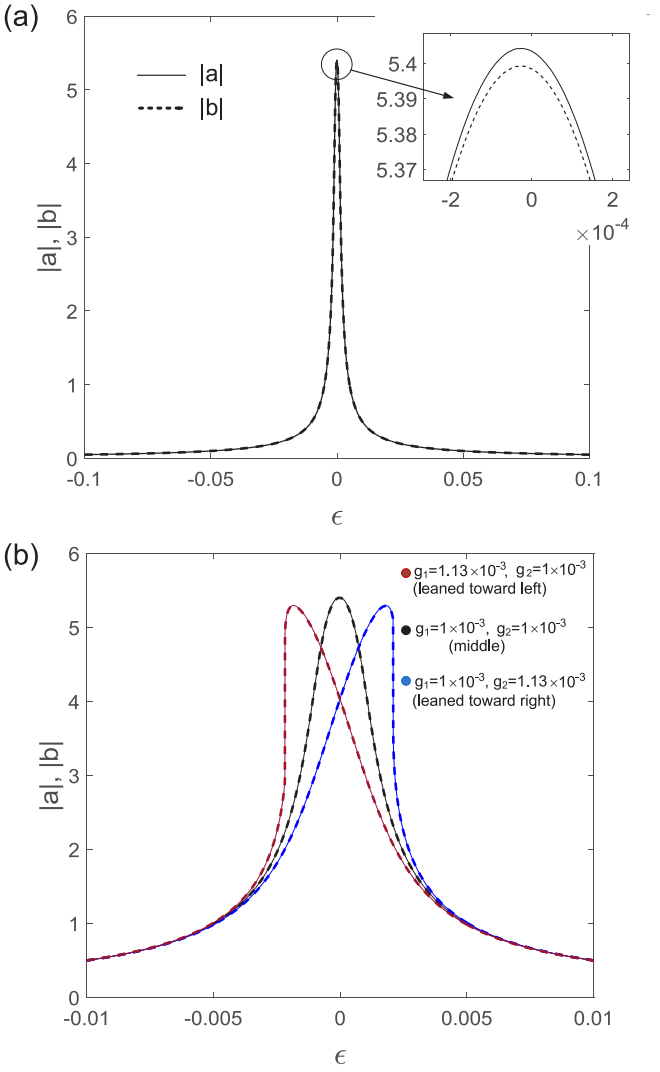

FIG. 7. Absolute value of mode amplitudes in the nonlinear case: (a) $g_1 = g_2 = 0.001$. (b) Tunability of the resonance for different values of Kerr coefficients.

amplitudes a and b can be calculated from Eq. (5) as

$$a = \frac{(-\Delta - \epsilon + g_2|b|^2 + i\delta)\eta s_i}{(-\Delta + \epsilon + g_1|a|^2 - i\delta)(-\Delta - \epsilon + g_2|b|^2 + i\delta) - \upsilon^2}, \tag{6a}$$

$$b = \frac{-\upsilon\eta s_i}{(-\Delta + \epsilon + g_1|a|^2 - i\delta)(-\Delta - \epsilon + g_2|b|^2 + i\delta) - \upsilon^2}, \tag{6b}$$

where $\Delta = \omega - \omega_0$. If we set the source frequency ω equal to ω_0 ($\Delta = 0$), Eq. (6) implies that, in the linear case ($g_1 = g_2 = 0$), EP conditions ($\epsilon = 0$, $\delta = \pm\upsilon$) cause the denominator of the mode amplitudes to become zero. However, in the nonlinear case ($g_1, g_2 \neq 0$), EP conditions would not make the denominator zero since the expression $(g_1|a|^2 - i\delta)(g_2|b|^2 + i\delta)$ (the complex value) cannot equal υ^2 (the real value).

Figure 7(a) shows the absolute value of the mode amplitudes $|a|$ and $|b|$ with respect to ϵ for $g_1 = g_2 = 0.001$, $\upsilon \approx \delta = 1$, $\Delta = 0$, and $\eta s_i = 0.01$. It is obtained by solving the matrix form of Eq. (5), numerically, with the same method as in Sec. II. In addition, for better convergence of the numerical method, we consider $\upsilon = 0.9995$, a value very close to 1. It depicts a resonance at $\epsilon = 0$, as in the linear case, at which the amplitude of the resonance is around 5.4, which is 540 times larger than the coupled source amplitude $\eta s_i = 0.01$. By decreasing the nonlinear coefficients g_1 and g_2, the amplitude of the resonance approaches infinity. However, even in the linear case, the experimental result shows that the EP condition in such systems leads to a finite, but large, value of the resonance in the transmission spectra [7]. The inset in Fig. 7(a) is related to the magnified $|a|$ and $|b|$, which are pretty close to each other around $\epsilon = 0$, as in the linear case.

Finally, Fig. 7(b) shows the tunability of the resonance associated with the EP conditions for different values of the nonlinear coefficients, which was previously predicted by solving the eigenvalue problem in Sec. II. Figure 7(b) reveals that with equal nonlinear coefficients, the resonance occurs at $\epsilon = 0$, while for unequal nonlinear coefficients, the resonance leans toward the left or right side.

V. PRACTICAL OUTLOOK

Due to the similarity between ring resonators and optical fibers, we investigate a practical value of the Kerr nonlinearity in optical fibers. By considering the spatial distribution of the field amplitude in an optical fiber containing a nonlinear material and applying the Helmholtz equation, the effect of a nonlinear material is evaluated with a small variation of the wave number within the perturbation approach [38]. The nonlinear coefficient is then estimated, $g(\omega_0) = \frac{n_2(\omega_0)\omega_0}{cA_{\text{eff}}}$, as the coefficient of the term $|A|^2A$, where n_2 is the nonlinear-index coefficient related to third-order susceptibility $\chi^{(3)}$, A_{eff} is the effective mode area, and ω_0 and A are the frequency and amplitude of the optical mode, respectively. In a more conventional form, g can be written as $g = \frac{2\pi n_2}{\lambda A_{\text{eff}}}$. We can consider the field amplitude A to be normalized such that $|A|^2$ represents the optical power, and n_2 is expressed in m^2/W; then the quantity $g|A|^2$ is measured in m^{-1} [to use this nonlinear coefficient in the temporal coupled-mode theory (CMT), we should multiply it by c/n, the ratio of the speed of light and (relative) refractive index of material—the conversion of the eigenwave number to eigenfrequency—and $g|A|^2$ would be in units of rad s^{-1}; however, in spatial CMT this conversion is not required].

Therefore, the nonlinear coefficient depends on the frequency, fiber design, and nonlinear material. As an example, for a fiber with a 2-μm core diameter, air as its cladding, silica as its core with (relative) refractive index $n = 1.45$, and nonlinear-index coefficient $n_2 \approx 2.6 \times 10^{-20}$ m^2/W, at a wavelength near $\lambda = 1$ μm, the nonlinear coefficient is estimated to be $g \approx 0.1$ W^{-1}/m.

On the other hand, to create loss or gain in the coupled resonators and waveguides, [7] proposed an active Er^+-doped silica microtoroid coupled to a passive silica microtoroid to provide optical gain, while in [6], optical loss was produced by a thin Cr layer deposited on a $\text{Al}_{0.2}\text{Ga}_{0.8}\text{As}$ planar waveguide coupled to a lossless $\text{Al}_{0.2}\text{Ga}_{0.8}\text{As}$ planar waveguide. In the notations of [6], the EP can happen when the loss

coefficient is 4 times the coupling rate, $\alpha = 4\upsilon$, which is around $\alpha = 900\ \mathrm{m}^{-1}$ at $\lambda = 1.55\ \mu\mathrm{m}$. However, in our notations, the EP can occur for a loss coefficient equal to the coupling rate, $\delta = \upsilon$. Therefore, we can consider $\delta = 225\ \mathrm{m}^{-1}$, according to our notations. If we assume, at a wavelength around $\lambda = 1\ \mu\mathrm{m}$, we can create almost half of this amount of loss in silica-based coupled resonators and fibers (since the refractive index of silica, $n = 1.45$, is almost half that of $Al_{0.2}Ga_{0.8}As$, $n = 3.28$), we can write $\delta \approx 100\ \mathrm{m}^{-1}$.

From the last two paragraphs, we can deduce that the ratio of some practical values of nonlinear and loss coefficients can be $g/\delta \approx 0.001$. In Fig. 7, we used the same ratio, $g/\delta \approx 0.001$, for the nonlinear and gain and loss values, while in the other figures, which deal with the eigenvalue problem, this ratio is much higher than 0.001. However, it does not violate the general concept of the paper, and tunability could be shown for any other values of nonlinear coefficients g. Furthermore, in the eigenvalue problem (unlike Fig. 7), the values $|a|^2$ and $|b|^2$ are smaller than unity since they represent the probability density of the energy levels; therefore, the nonlinear coefficients in the terms $g_1|a|^2a$ and $g_2|b|^2b$ are chosen to be large enough to show the tunability effectively.

VI. CONCLUSION

We observed that both second- and third-order EPs can be tuned by the contrast between the Kerr nonlinearities in the matrix equation. Furthermore, near the EP, the real parts of the eigenvalues coincide, while their imaginary parts depart. The distance between these points and the EP can also be tuned by a nonlinear coefficient. Meanwhile, we showed that with Kerr nonlinearity, the absolute value of the mode amplitude in the ideal $\mathcal{PT}$-symmetric system can lean toward the right or left side with respect to the parameter space ϵ. To solve the nonlinear non-Hermitian eigenvalue problem, we proposed a numerical method based on self-consistent-field and iteration methods in two stages: first, we calculate eigenvalues with respect to ϵ, from large to small values of $|\epsilon|$. Second, the discontinuities from the previous stage are removed by defining additional parameters for the eigenfunctions so that the changing rate of the eigenfunctions is preserved.

ACKNOWLEDGMENTS

We are grateful to J. Wiersig at OVGU for helpful discussions. The work is supported by the Russian Science Foundation (Project No. 21-12-00383).

[1] M. A. Miri and A. Alu, Exceptional points in optics and photonics, Science **363** (2019).

[2] H. Hodaei, M.-A. Miri, M. Heinrich, D. N. Christodoulides, and M. Khajavikhan, Parity-time-symmetric microring lasers, Science **346**, 975 (2014).

[3] H. Hodaei, A. U. Hassan, S. Wittek, H. Garcia-Gracia, R. El-Ganainy, D. N. Christodoulides, and M. Khajavikhan, Enhanced sensitivity at higher-order exceptional points, Nature (London) **548**, 187 (2017).

[4] C. M. Bender and S. Boettcher, Real Spectra in Non-Hermitian Hamiltonians Having $\mathcal{PT}$ Symmetry, Phys. Rev. Lett. **80**, 5243 (1998).

[5] D. Christodoulides and J. Yang, *Parity-time Symmetry and Its Applications*, Springer Tracts in Modern Physics Vol. 280 (Springer, Singapore, 2018).

[6] A. Guo, G. J. Salamo, D. Duchesne, R. Morandotti, M. Volatier-Ravat, V. Aimez, G. A. Siviloglou, and D. N. Christodoulides, Observation of $\mathcal{PT}$-Symmetry Breaking in Complex Optical Potentials, Phys. Rev. Lett. **103**, 093902 (2009).

[7] B. Peng, S. K. Özdemir, F. Lei, F. Monifi, M. Gianfreda, G. L. Long, S. Fan, F. Nori, C. M. Bender, and L. Yang, Parity-time-symmetric whispering-gallery microcavities, Nat. Phys. **10**, 394 (2014).

[8] E. M. Graefe and H. J. Korsch, Crossing scenario for a nonlinear non-Hermitian two-level system, Czech. J. Phys. **56**, 1007 (2006).

[9] D. Witthaut, E. M. Graefe, S. Wimberger, and H. J. Korsch, Bose-Einstein condensates in accelerated double-periodic optical lattices: Coupling and crossing of resonances, Phys. Rev. A **75**, 013617 (2007).

[10] D. Cartarius, J. Main, and G. Wunner, Discovery of exceptional points in the Bose-Einstein condensation of gases with attractive $1/r$ interaction, Phys. Rev. A **77**, 013618 (2008).

[11] G. Wunner, H. Cartarius, P. Koberle, J. Main, and S. Rau, Exceptional points for nonlinear Schroedinger equations describing Bose-Einstein condensates of ultracold atomic gases, Acta Polytechnica **51**, 95 (2011).

[12] P. Köberle, H. Cartarius, T. Fabcic, J. Main, and G. Wunner, Bifurcations, order and chaos in the Bose-Einstein condensation of dipolar gases, New J. Phys. **11**, 023017 (2009).

[13] P. Djorwe, Y. Pennec, and B. Djafari-Rouhani, Frequency locking and controllable chaos through exceptional points in optomechanics, Phys. Rev. E **98**, 032201 (2018).

[14] H. Hashemi, A. W. Rodriguez, J. D. Joannopoulos, M. Soljačić, and S. G. Johnson, Nonlinear harmonic generation and devices in doubly resonant Kerr cavities, Phys. Rev. A **79**, 013812 (2009).

[15] K. Li and P. G. Kevrekidis, $\mathcal{PT}$-symmetric oligomers: Analytical solutions, linear stability, and nonlinear dynamics, Phys. Rev. E **83**, 066608 (2011).

[16] E.-M. Graefe, H. J. Korsch, and A. E. Niederle, Quantum-classical correspondence for a non-Hermitian Bose-Hubbard dimer, Phys. Rev. A **82**, 013629 (2010).

[17] E.-M. Graefe, Stationary states of a PT symmetric two-mode Bose-Einstein condensate, J. Phys. A **45**, 444015 (2012).

[18] H. Ramezani and T. Kottos, Unidirectional nonlinear $\mathcal{PT}$-symmetric optical structures, Phys. Rev. A **82**, 043803 (2010).

[19] E. M. Graefe, U. Günther, H. J. Korsch, and A. E. Niederle, A non-Hermitian $\mathcal{PT}$ symmetric Bose-Hubbard model: Eigenvalue rings from unfolding higher-order exceptional points, J. Phys. A **41**, 255206 (2008).

[20] M. Y. Nada, M. A. K. Othman, and F. Capolino, Theory of coupled resonator optical waveguides exhibiting high-order exceptional points of degeneracy, Phys. Rev. B **96**, 184304 (2017).

[21] W. Chen, S. K. Özdemir, G. Zhao, J. Wiersig, and L. Yang, Exceptional points enhance sensing in an optical microcavity, Nature (London) **548**, 192 (2017).

[22] M. Witzany, T.-L. Liu, J.-B. Shim, F. Hargart, E. Koroknay, W.-M. Schulz, M. Jetter, E. Hu, J. Wiersig, and P. Michler, Strong mode coupling in InP quantum dot-based GaInP microdisk cavity dimers, New J. Phys. **15**, 013060 (2013).

[23] M. Benyoucef, J.-B. Shim, J. Wiersig, and O. G. Schmidt, Quality-factor enhancement of supermodes in coupled microdisks, Opt. Lett. **36**, 1317 (2011).

[24] A. U. Hassan, H. Hodaei, M.-A. Miri, M. Khajavikhan, and D. N. Christodoulides, Nonlinear reversal of the $\mathcal{PT}$-symmetric phase transition in a system of coupled semiconductor microring resonators, Phys. Rev. A **92**, 063807 (2015).

[25] S. Malzard, E. Cancellieri, and H. Schomerus, Topological dynamics and excitations in lasers and condensates with saturable gain or loss, Opt. Express **26**, 22506 (2018).

[26] W. Langbein, No exceptional precision of exceptional-point sensors, Phys. Rev. A **98**, 023805 (2018).

[27] H. Wang, Y.-H. Lai, Z. Yuan, M.-G. Suh, and K. Vahala, Petermann-factor sensitivity limit near an exceptional point in a Brillouin ring laser gyroscope, Nat. Commun. **11**, 1610 (2020).

[28] M. Zhang, W. Sweeney, C. W. Hsu, Lan Yang, A. D. Stone, and L. Jiang, Quantum Noise Theory of Exceptional Point Amplifying Sensors, Phys. Rev. Lett. **123**, 180501 (2019).

[29] J. Wiersig, Robustness of exceptional-point-based sensors against parametric noise: The role of Hamiltonian and Liouvillian degeneracies, Phys. Rev. A **101**, 053846 (2020).

[30] J. Wiersig, Prospects and fundamental limits in exceptional point-based sensing, Nat. Commun. **11**, 2454 (2020).

[31] E. M. Graefe, H. J. Korsch, and A. E. Niederle, Mean-Field Dynamics of a Non-Hermitian Bose-Hubbard Dimer, Phys. Rev. Lett. **101**, 150408 (2008).

[32] H. Haus and W. Huang, Coupled-mode theory, Proc. IEEE **79**, 1505 (1991).

[33] A. Rodriguez, M. Soljacic, J. D. Joannopoulos, and S. G. Johnson, $\chi^{(2)}$ and $\chi^{(3)}$ harmonic generation at a critical power in inhomogeneous doubly resonant cavities, Opt. Express **15**, 7303 (2007).

[34] D. R. Hartree, The wave mechanics of an atom with a non-Coulomb central field. Part II. Some results and discussion, Math. Proc. Cambridge Philos. Soc. **24**, 111 (1928).

[35] B. Wu and Q. Niu, Nonlinear Landau-Zener tunneling, Phys. Rev. A **61**, 023402 (2000).

[36] A. K. Burnham, L. W. Buxton, and W. H. Flygare, Kerr constants, depolarization ratios, and hyperpolarizabilities of substituted methanes, J. Chem. Phys. **67**, 4990 (1977).

[37] Z. Xiao, H. Li, T. Kottos, and A. Alù, Enhanced Sensing and Nondegraded Thermal Noise Performance Based on $\mathcal{PT}$-Symmetric Electronic Circuits with a Sixth-Order Exceptional Point, Phys. Rev. Lett. **123**, 213901 (2019).

[38] G. P. Agrawal, in *Nonlinear Fiber Optics*, 4th ed. (Academic Press, USA, 2007), Chap. 2, 11.